International Journal of Control, Automation, and Systems 22(8) (2024) 2494-2503
http://dx.doi.org/10.1007/s12555-023-0510-8
ISSN:1598-6446 eISSN:2005-4092
http://www.springer.com/12555

Augmented Proportional and Integral Observer Design for Fault Estimation in Discrete-time Systems With Applications to Wind Turbine Systems and Electro-mechanical Servo Systems

Zikang Li, Zhi-Wei Gao*, and Yuanhong Liu

Abstract: In this paper, a fault estimation technique is addressed to simultaneously estimate system states, actuator, and sensor faults for discrete-time dynamic systems. Specifically, an augmented system is constructed by defining an extended state vector composed of original system states and actuator faults. For this augmented system, an augmented proportional and integral observer is addressed to simultaneously estimate system states, actuator faults as well sensor faults for a discrete-time linear system. A robust augmented proportional and integral observer is designed for Lipschitz nonlinear systems subjected to unknown input uncertainties. The proposed approaches are applied to wind turbine drive train system and electro-mechanical servo system for the validation, which have shown satisfactory estimation performance.

Keywords: Augmented proportional and integral observer, augmented systems, electro-mechanical servo system, fault estimation, Lipschitz nonlinear systems, wind turbine.

1. INTRODUCTION

In an industrial process or industrial automation system, the system or component is prone to faults due to age or unexpected reasons. A fault is defined as an unexpected deviation from the normal system characteristics, which could cause further damage or accidence if the fault was not detected at early stages and no corresponding actions were taken. Information redundancy-based fault diagnosis approaches can be categorized into model-based approach, signal-based method, and knowledge-based techniques [1,2]. Fault diagnosis generally includes three tasks such as fault detection, fault isolation and fault identification. The model-based approach has been a powerful tool if the system model is available to the designers, and observer-based fault detection approach plays an important role for fault detection and diagnosis [3,4]. Fault estimation has proven a powerful tool for fault diagnosis, which was initiated in 2000s, which can determine the size and shape of the fault concerned [5,6]. In recent years, there have been increasing solutions to fault estimation problems [7-12]. Fault estimators include adaptive estimator [13-15], sliding-mode observer [10,16,17], proportional-integral observer [5,18,19], augmented observer [20,21] and descriptor observer [6,22,23].

Lipschitz nonlinear systems are an interesting topic which has received much attention. For a class of unilateral Lipschitz systems, a sensor fault observer was presented using linear matrix inequality approach [24]. A robust fault estimation approach was proposed in the work by Kazemi *et al.* [25] for nonlinear Lipschitz systems by maximizing Lipschitz constant and minimizing disturbance attenuation level. In [26], two sliding-mode observers were designed to estimate actuator and sensor faults respectively for uncertain Lipschitz nonlinear systems. By combining a generalized observer and an adaptive sliding mode observer, a fault reconstruction method was addressed in [27] to reconstruct both sensor and actuator faults where the effects of uncertainty and Lipschitz nonlinearity were attenuated. In [28], a robust fault estimation technique was proposed to deal with Lipschitz nonlinear systems subjected to process and sensor disturbances using unknown input observers for decoupling and attenuating unknown input uncertainties.

It is noticed that most of the results above are focused on continuous systems, which are not applicable to discrete-time systems. The discrete-time results of fault and disturbance estimates can be found in the

Manuscript received August 7, 2023; revised January 5, 2024; accepted February 15, 2024. Recommended by Associate Editor Gyujin Na under the direction of Senior Editor Sangmoon Lee. The authors would like to thank the support from the Starting Research Fund for Talents, Touyan Research Grant in Northeast Petroleum University and the Fundamental Research Grant of Heilongjiang Province (2023TSTD-03).

Zikang Li, Zhi-Wei Gao, and Yuanhong Liu are with the Research Centre for Digitalization and Intelligent Diagnosis to New Energies, College of Electrical and Information Engineering, Northeast Petroleum University, Daqing, 163000, China (e-mails: lzk570966920@163.com, {gaozhiwei, liuyuanhong}@nepu.edu.cn).
* Corresponding author.

literature, e.g., in [18,29-32]. Specifically, discrete-time proportional-integral observer designs were respectively addressed by [18,29] for linear dynamic systems. For Lipschitz nonlinear systems, a descriptor augmented observer approach was presented to simultaneously estimate system states and unanticipated perturbations caused by unknow sensor delays in [30]. In [31], descriptor augmented system approach and unknow input proportional-integral observer were combined to investigate fault estimation problem for discrete-time nonlinear systems. In [32], an augmented unknown input observer was designed to estimate faults for both linear and Lipschitz nonlinear systems and achieve robustness by decoupling unknown input uncertainties.

Compared with the fruitful results of continuous systems, the results of fault estimation approaches for discrete-time dynamic systems are relatively few. Motivated by the above, in this study, we will revisit the fault estimate problem by using an alternative approach. This paper aims to provide robust state and fault estimates for discrete-time dynamic systems subjected to unknown input perturbations and potential actuator and sensor faults. Firstly, an augmented system is constructed by defining an augmented state vector composed of system states and actuator faults. Secondly, a proportional-integral observer is applied to the augmented system for estimating system sensor faults. The contributions of this paper are as follows:

1) The estimator can accurately estimate the state, actuator fault, and sensor fault for linear discrete-time systems.
2) The estimator can robustly estimate the state, actuator fault, and sensor fault for discrete-time systems in the presence of unknown input disturbance and Lipschitz nonlinearity.
3) The gains of the robust estimator are obtained by solving linear matrix inequality.
4) The upper limits of the unknown input uncertainties, actuator and sensor faults do not need to be known for the design.
5) Compared with the augmented discrete-time unknown-input observer designed by [32], this estimator in the proposed design does not need to satisfy the disturbance decoupling condition, which may suit a wider application of industrial systems.
6) The proposed fault estimation approaches are applied to a wind turbine drive-train system and an electromechanical servo system for the validation, which will benefit predictive maintenance for improving the reliability, safety, and availability of the industrial systems.

This article is structured as follows: Section 2 addresses a design approach for fault estimation for linear discrete-time dynamic systems using augmented proportional-integral observer. In Section 3, the fault estimator is extended to Lipschitz nonlinear discrete-time systems with unknown input disturbances to estimate state, actuator, and sensor faults. In Section 4, two engineering-oriented systems (wind turbine drive train system and electromechanical servo system) are used to verify the effectiveness of the method. The paper is ended by the conclusion.

2. STATE AND FAULT ESTIMATOR FOR LINEAR DISCRETE-TIME SYSTEMS

Consider the following discrete dynamic linear system

$$x(k+1) = Ax(k) + Bu(k) + E_a f_a(k), \tag{1}$$
$$y(k) = Cx(k) + E_s f_s(k), \tag{2}$$

where $x(k) \in R^n$ is the state vector, $u(k) \in R^m$ is the control input vector, $y(k) \in R^p$ is the measured output vector, $f_a \in R^q$ is the actuator fault, $f_s \in R^r$ is the sensor fault. A, B, C, E_a, and E_s are known matrices with appropriate dimensions, respectively. Clearly, $x(k)$ is a simplified representation of $x(kT_s)$, where T_s is the sampling interval.

Motivated by [18,29], we have Assumption 1.

Assumption 1: The sampling interval T_s is sufficiently small such that the fault does not vary too much between two consecutive sample instances. In this case, one can have

$$f_a(k+1) - f_a(k) = \Delta_a(k), \tag{3}$$
$$f_s(k+1) - f_s(k) = \Delta_s(k), \tag{4}$$

which has a magnitude of the order $O(T_s^2)$ for all k.

Assumption 2 below is also useful for the observer design.

Assumption 2: The pair (A, C) is observable, and

$$rank \begin{bmatrix} A - I_n & E_a & 0 \\ C & 0 & E_s \end{bmatrix} = n + q + r. \tag{5}$$

Let $\bar{x}(k) = \begin{bmatrix} x(k)^T & f_a(k)^T \end{bmatrix}^T$. We can establish an augmentation system as follows:

$$\bar{x}(k+1) = \bar{A}\bar{x}(k) + \bar{B}u(k) + \bar{E}\Delta_a(k), \tag{6}$$
$$y(k) = \bar{C}\bar{x}(k) + E_s f_s(k), \tag{7}$$

where

$$\bar{A} = \begin{bmatrix} A & E_a \\ 0 & I_q \end{bmatrix}, \bar{B} = \begin{bmatrix} B \\ 0 \end{bmatrix}, \bar{E} = \begin{bmatrix} 0 \\ I_q \end{bmatrix}, \bar{C} = \begin{bmatrix} C & 0 \end{bmatrix}.$$

Based on the state space equations (6) and (7), the following forms of augmented observers can be designed

$$\hat{\bar{x}}(k+1) = \bar{A}\hat{\bar{x}}(k) + \bar{B}u(k) + L\left[y(k) - \hat{y}(k)\right], \tag{8}$$
$$\hat{f}_s(k+1) = \hat{f}_s(k) + K\left[y(k) - \hat{y}(k)\right], \tag{9}$$

$$\hat{y}(k) = \bar{C}\hat{\bar{x}}(k) + E_s\hat{f}_s(k), \tag{10}$$

where $\hat{\bar{x}} \in R^{n+q}$ is the estimation of augmented state vector, $\hat{f}_s \in R^r$ is the estimation of the sensor fault, $L \in R^{(n+q)\times p}$ and $K \in R^{r\times p}$ are the proportional and integral gains, respectively.

Theorem 1: Under Assumptions 1 and 2, for discrete augmented state-space systems (6) and (7), there are observers in the form of (8)-(10), so that the state and fault estimation errors are constrained within a small range of $O(T_s^2)$.

Proof: Let $\bar{e}_x(k) = \bar{x}(k) - \hat{\bar{x}}(k)$ and $e_{f_s}(k) = f_s(k) - \hat{f}_s(k)$. In terms of (6)-(9), we can have the estimation errors as follows:

$$\begin{aligned}\bar{e}_x(k+1) &= \bar{x}(k+1) - \hat{\bar{x}}(k+1)\\ &= (\bar{A} - L\bar{C})\bar{e}_x(k) - LE_s e_{f_s}(k) + \bar{E}\Delta_a(k),\end{aligned} \tag{11}$$

$$\begin{aligned}e_{f_s}(k+1) &= f_s(k+1) - \hat{f}_s(k+1)\\ &= f_s(k+1) - \hat{f}_s(k) - K[y(k) - \hat{y}(k)]\\ &= -K\bar{C}\bar{e}_x(k) + (I - KE_s)e_{f_s}(k) + \Delta_s(k).\end{aligned} \tag{12}$$

From (11) and (12), the error dynamic equation can be obtained

$$\bar{e}(k+1) = \tilde{A}\bar{e}(k) + \bar{\bar{E}}\bar{\bar{\Delta}}(k), \tag{13}$$

where

$$\bar{e}(k) = \begin{bmatrix}\bar{e}_x(k)\\ e_{f_s}(k)\end{bmatrix},\ \tilde{A} = \bar{\bar{A}} - \bar{\bar{K}}\bar{\bar{C}},\ \bar{\bar{A}} = \begin{bmatrix}\bar{A} & 0\\ 0 & I_r\end{bmatrix},$$
$$\bar{\bar{K}} = \begin{bmatrix}L\\ K\end{bmatrix},\ \bar{\bar{C}} = \begin{bmatrix}\bar{C} & E_s\end{bmatrix},\ \bar{\bar{E}} = \begin{bmatrix}\bar{E} & 0\\ 0 & I_r\end{bmatrix},\ \bar{\bar{\Delta}}(k) = \begin{bmatrix}\Delta_a(k)\\ \Delta_s(k)\end{bmatrix}.$$

Observe that for any complex number z,

$$\begin{aligned}&rank\begin{bmatrix}zI_{n+q+r} - \bar{\bar{A}}\\ \bar{\bar{C}}\end{bmatrix}\\ &= rank\begin{bmatrix}zI_{n+q} - \bar{A} & 0\\ 0 & zI_r - I_r\\ \bar{C} & E_s\end{bmatrix}\\ &= rank\begin{bmatrix}zI_n - A & -E_a & 0\\ 0 & zI_q - I_q & 0\\ 0 & 0 & zI_r - I_r\\ C & 0 & E_s\end{bmatrix}\\ &= \begin{cases} rank\begin{bmatrix}zI_n - A\\ C\end{bmatrix} + q + r, & z \neq 1,\\ rank\begin{bmatrix}A - I_n & E_a & 0\\ C & 0 & E_s\end{bmatrix}, & z = 1.\end{cases}\end{aligned} \tag{14}$$

If Assumption 2 is true, we can conclude that $(\bar{\bar{A}}, \bar{\bar{C}})$ is observable according to (14). Therefore, a gain $\bar{\bar{K}}$ can be found to make $\bar{\bar{A}} - \bar{\bar{K}}\bar{\bar{C}}$ stable. If $\bar{\bar{\Delta}}(k)$ in (13) is null, one can find $\bar{e}_x(k) \to 0$ and $e_{f_s}(k) \to 0$ when $k \to \infty$. According to Assumption 1, $\Delta_a(k) \in O(T_s^2)$ and $\Delta_s(k) \in O(T_s^2)$, which means that the estimation error can be limited to a small region of $O(T_s^2)$. This completes the proof. □

Remark 1: An augmented proportional-integral observer is addressed in Theorem 1, which is used to estimate the system state, actuator fault and sensor fault at the same time. In the papers [18,29], the input disturbance and output disturbances are in the same forms, which can be estimated by a proportional-integral discrete-time observer. In Theorem 1, the actuator fault and sensor fault are characterized by respective signals, which are estimated by combining augmented system approach and a proportional-integral observer.

3. STATE AND FAULT ESTIMATOR FOR LIPSCHITZ SYSTEMS

Consider the following Lipschitz nonlinear system subjected to process disturbances

$$\begin{aligned}x(k+1) &= Ax(k) + Bu(k) + E_a f_a(k) + Dd(k)\\ &\quad + \psi[x(k),\ u(k)],\end{aligned} \tag{15}$$
$$y(k) = Cx(k) + E_s f_s(k), \tag{16}$$

where $d(k)$ is the unknown input disturbance, and $\psi[x(k), u(k)]$ is a Lipschitz nonlinear function, and the other symbols are defined as before.

Assumption 3: The nonlinear term $\psi[x(k), u(k)]$ is local Lipschitz relative to x in a region containing the origin, and is consistent in u, that is

$$\|\psi[x(k),\ u(k)] - \psi[\hat{x}(k),\ u(k)]\| \leq \gamma\|x(k) - \hat{x}(k)\|. \tag{17}$$

Let $\bar{x}(k) = \begin{bmatrix}x(k)^T & f_a(k)^T\end{bmatrix}^T$, then one has

$$\begin{aligned}\bar{x}(k+1) &= \bar{A}\bar{x}(k) + \bar{B}u(k) + \bar{D}\bar{d}(k)\\ &\quad + M\psi[x(k),\ u(k)],\end{aligned} \tag{18}$$
$$y(k) = \bar{C}\bar{x}(k) + E_s f_s(k), \tag{19}$$

where

$$M = \begin{bmatrix}I_n\\ 0\end{bmatrix},\ \bar{A} = \begin{bmatrix}A & E_a\\ 0 & I_q\end{bmatrix},\ \bar{B} = \begin{bmatrix}B\\ 0\end{bmatrix},$$
$$\bar{C} = \begin{bmatrix}C & 0\end{bmatrix},\ \bar{D} = \begin{bmatrix}D & 0\\ 0 & I_q\end{bmatrix},\ \bar{d}(k) = \begin{bmatrix}d(k)\\ \Delta_a(k)\end{bmatrix}.$$

According to (18) and (19), the observer is designed as follows:

$$\begin{aligned}\hat{\bar{x}}(k+1) &= \bar{A}\hat{\bar{x}}(k) + \bar{B}u(k) + M\psi[\hat{x}(k),\ u(k)]\\ &\quad + L[y(k) - \hat{y}(k)],\end{aligned} \tag{20}$$
$$\hat{f}_s(k+1) = \hat{f}_s(k) + K[y(k) - \hat{y}(k)], \tag{21}$$

$$\hat{y}(k) = \bar{C}\hat{\bar{x}}(k) + E_s\hat{f}_s(k). \tag{22}$$

Using (18)-(20), the estimation error equations are given as follows:

$$\begin{aligned}\bar{e}_x(k+1) &= (\bar{A} - L\bar{C})\bar{e}_x(k) - LE_s e_{f_s}(k) + \bar{D}\bar{d}(k) \\ &\quad + M\Psi(k), \end{aligned} \tag{23}$$

$$e_{f_s}(k+1) = -K\bar{C}\bar{e}_x(k) + (I - KE_s)e_{f_s}(k) + \Delta_s(k), \tag{24}$$

where

$$\Psi(k) = \psi[x(k),\, u(k)] - \psi[\hat{x}(k),\, u(k)]. \tag{25}$$

The error dynamic equation can be obtained from (23) and (24)

$$\bar{e}(k+1) = \tilde{A}\bar{e}(k) + \bar{\bar{D}}\bar{\bar{d}}(k) + \bar{M}\Psi(k), \tag{26}$$

where

$$\bar{e}(k) = \begin{bmatrix} \bar{e}_x(k) \\ e_{f_s}(k) \end{bmatrix},\ \tilde{A} = \bar{\bar{A}} - \bar{\bar{K}}\bar{\bar{C}},\ \bar{\bar{A}} = \begin{bmatrix} \bar{A} & 0 \\ 0 & I_r \end{bmatrix},$$

$$\bar{\bar{K}} = \begin{bmatrix} L \\ K \end{bmatrix},\ \bar{\bar{C}} = \begin{bmatrix} \bar{C} & E_s \end{bmatrix},\ \bar{\bar{D}} = \begin{bmatrix} \bar{D} & 0 \\ 0 & I_r \end{bmatrix},$$

$$\bar{\bar{d}}(k) = \begin{bmatrix} \bar{d}(k) \\ \Delta_s(k) \end{bmatrix},\ \bar{M} = \begin{bmatrix} M \\ 0 \end{bmatrix}.$$

Lemma 1 [25]**:** Let $X \in R^{s\times t}$, $Y \in R^{t\times s}$, and $F \in R^{t\times t}$, where F satisfies $F^TF \le I$; $x \in R^s$ and $y \in R^s$. For any scalar $\alpha > 0$, the following inequality holds

$$2x^TXFYy \le \frac{1}{\alpha}x^TXX^Tx + \alpha y^TY^TYy. \tag{27}$$

The design goal here is to ensure system (26) to be robustly stable against the effect from the disturbance $\bar{\bar{d}}(k)$, that is,

$$\bar{e}(k)_2 < \mu\bar{\bar{d}}(k)_2, \tag{28}$$

where

$$\begin{cases} \bar{e}(k)_2 = \left(\sum\limits_{k=0}^{\infty} \bar{e}^T(k)\bar{e}(k)\right)^{\frac{1}{2}}, \\ \bar{\bar{d}}(k)_2 = \left(\sum\limits_{k=0}^{\infty} \bar{\bar{d}}^T(k)\bar{\bar{d}}(k)\right)^{\frac{1}{2}}. \end{cases} \tag{29}$$

For realizing this goal, the following theorem is given.

Theorem 2: If there is a symmetric positive definite matrix $P \in R^{(n+q+r)\times(n+q+r)}$, the appropriate matrix $U \in R^{(n+q+r)\times(q+r)}$ and a scalar $\mu > 0$, so that the following linear matrix inequalities (LMI) hold

$$\begin{bmatrix} \Omega & 0 & \bar{\bar{A}}^TP - \bar{\bar{C}}^TU^T & \tilde{A}^TP & 0 \\ * & -\mu I & \bar{\bar{D}}^TP & 0 & \bar{\bar{D}}^TP \\ * & * & -P & 0 & 0 \\ * & * & * & -I & 0 \\ * & * & * & * & -I \end{bmatrix} < 0, \tag{30}$$

the error dynamic system (26) is robustly stable, which means the observer (20)-(22) can simultaneously estimate the state vector, actuator fault, and sensor fault in Lipschitz nonlinear system systems (15) and (16). In (30), $\Omega = -P + 2\bar{\bar{M}}^T\bar{\bar{M}} + \bar{\bar{M}}^TP\bar{\bar{M}} + \frac{1}{\mu}I$, $\bar{\bar{M}} = \begin{bmatrix} \gamma\bar{M} & 0_{n+q+r,q} & 0_{n+q+r,r} \end{bmatrix}$, and the observer gain can be calculated by $\bar{\bar{K}} = P^{-1}U$.

Proof: Let the Lyapunov function

$$V(k) = \bar{e}^T(k)P\bar{e}(k). \tag{31}$$

Then we have

$$\begin{aligned} &\Delta V(k) \\ &= V(k+1) - V(k) \\ &= \bar{e}^T(k+1)P\bar{e}(k+1) - \bar{e}^T(k)P\bar{e}(k) \\ &= \bar{e}^T(k)\tilde{A}^TP\tilde{A}\bar{e}(k) + \bar{\bar{d}}^T(k)\bar{\bar{D}}^TP\bar{\bar{D}}\bar{\bar{d}}(k) \\ &\quad + \Psi^T(k)\bar{M}^TP\bar{M}\Psi(k) + 2\bar{e}^T(k)\tilde{A}^TP\bar{\bar{D}}\bar{\bar{d}}(k) \\ &\quad + 2\bar{e}^T(k)\tilde{A}^TP\bar{M}\Psi(k) + 2\bar{\bar{d}}^T(k)\bar{\bar{D}}^TP\bar{M}\Psi(k) \\ &\quad - \bar{e}^T(k)P\bar{e}(k). \end{aligned} \tag{32}$$

Using (27) and (17), we can obtain

$$\begin{aligned} 2\bar{e}^T(k)\tilde{A}^TP\bar{M}\Psi(k) &\le \bar{e}^T(k)\tilde{A}^TPP\tilde{A}\bar{e}(k) \\ &\quad + \Psi(k)^T\bar{M}^T\bar{M}\Psi(k), \end{aligned} \tag{33}$$

$$\begin{aligned} 2\bar{\bar{d}}^T(k)\bar{\bar{D}}^TP\bar{M}\Psi(k) &\le \bar{\bar{d}}^T(k)\bar{\bar{D}}^TPP\bar{\bar{D}}\bar{\bar{d}}(k) \\ &\quad + \Psi(k)^T\bar{M}^T\bar{M}\Psi(k), \end{aligned} \tag{34}$$

$$\Psi^T(k)\bar{M}^TP\bar{M}\Psi(k) \le \gamma^2 {e_x}^T(k)\bar{M}^TP\bar{M}e_x(k), \tag{35}$$

where $e_x(k) = x(k) - \hat{x}(k)$.

Substituting (33)-(35) in to (32), we have

$$\begin{aligned} &\Delta V(k) \\ &\le \bar{e}^T(k)\tilde{A}^TP\tilde{A}\bar{e}(k) + \bar{\bar{d}}^T(k)\bar{\bar{D}}^TP\bar{\bar{D}}\bar{\bar{d}}(k) \\ &\quad + 2\bar{e}^T(k)\tilde{A}^TP\bar{\bar{D}}\bar{\bar{d}}(k) + \gamma^2 {e_x}^T(k)\bar{M}^TP\bar{M}e_x(k) \\ &\quad + \bar{e}^T(k)\tilde{A}^TPP\tilde{A}\bar{e}(k) + \bar{\bar{d}}^T(k)\bar{\bar{D}}^TPP\bar{\bar{D}}\bar{\bar{d}}(k) \\ &\quad + 2\Psi(k)^T\bar{M}^T\bar{M}\Psi(k) - \bar{e}^T(k)P\bar{e}(k) \\ &= \bar{e}^T(k)\left(\tilde{A}^TP\tilde{A} + \tilde{A}^TPP\tilde{A} - P\right)\bar{e}(k) \\ &\quad + \bar{\bar{d}}^T(k)\left(\bar{\bar{D}}^TP\bar{\bar{D}} + \bar{\bar{D}}^TPP\bar{\bar{D}}\right)\bar{\bar{d}}(k) \\ &\quad + 2\bar{e}^T(k)\tilde{A}^TP\bar{\bar{D}}\bar{\bar{d}}(k) + \gamma^2 e_x^T\bar{M}^TP\bar{M}e_x \\ &\quad + 2\Psi(k)^T\bar{M}^T\bar{M}\Psi(k). \end{aligned} \tag{36}$$

Noticing that $\bar{\bar{M}} = \begin{bmatrix} \gamma\bar{M} & 0_{n+q+r,q} & 0_{n+q+r,r} \end{bmatrix}$ we can get $\gamma^2 e_x^T\bar{M}^TP\bar{M}e_x = \bar{e}^T(k)\bar{\bar{M}}^TP\bar{\bar{M}}\bar{e}(k)$. Therefore, we can have

$$\begin{aligned} &\Delta V(k) \\ &\le \bar{e}^T(k)\left(\Omega_1 - P + \bar{\bar{M}}^TP\bar{\bar{M}}\right)\bar{e}(k) \end{aligned}$$

$$
\begin{aligned}
&+\bar{\bar{d}}^T(k)\left(\bar{\bar{D}}^T P\bar{\bar{D}}+\bar{\bar{D}}^T PP\bar{\bar{D}}\right)\bar{\bar{d}}(k) \\
&+2\bar{e}^T(k)\tilde{A}^T P\bar{\bar{D}}\bar{\bar{d}}(k)+2\gamma^2 e_x^T(k)\bar{M}^T\bar{M}e_x(k) \\
=&\ \bar{e}^T(k)(\Omega_1+\Omega)\bar{e}(k) \\
&+\bar{\bar{d}}^T(k)\left(\bar{\bar{D}}^T P\bar{\bar{D}}+\bar{\bar{D}}^T PP\bar{\bar{D}}\right)\bar{\bar{d}}(k) \\
&+2\bar{e}^T(k)\tilde{A}^T P\bar{\bar{D}}\bar{\bar{d}}(k)-\frac{1}{\mu}\bar{e}^T(k)\bar{e}(k)+\mu\bar{\bar{d}}^T(k)\bar{\bar{d}}(k) \\
=&\begin{bmatrix}\bar{e}^T(k)\\ \bar{\bar{d}}^T(k)\end{bmatrix}^T\begin{bmatrix}\Omega_1+\Omega & \tilde{A}^T P\bar{\bar{D}}\\ * & \Omega_2\end{bmatrix}\begin{bmatrix}\bar{e}(k)\\ \bar{\bar{d}}(k)\end{bmatrix},
\end{aligned} \tag{37}
$$

where $\Omega_1 = \tilde{A}^T P\tilde{A} + \tilde{A}^T PP\tilde{A}$, and $\Omega_2 = \bar{\bar{D}}^T P\bar{\bar{D}} + \bar{\bar{D}}^T PP\bar{\bar{D}} - \mu I$.

Let us discuss the condition to ensure the following inequality to hold

$$
\begin{bmatrix}\Omega_1+\Omega & \tilde{A}^T P\bar{\bar{D}}\\ * & \Omega_2\end{bmatrix}<0, \tag{38}
$$

which is equivalent to the following

$$
\begin{aligned}
&\begin{bmatrix}\Omega+\tilde{A}^T PP\tilde{A} & 0\\ * & \bar{\bar{D}}^T PP\bar{\bar{D}}-\mu I\end{bmatrix} \\
&-\begin{bmatrix}\tilde{A}^T P\\ \bar{\bar{D}}^T P\end{bmatrix}(-P)^{-1}\begin{bmatrix}P\tilde{A} & P\bar{\bar{D}}\end{bmatrix}<0.
\end{aligned}
$$

Using the well-known Schur complement theorem, the equation above can be transformed into

$$
\begin{bmatrix}\tilde{A}^T PP\tilde{A}+\Omega & 0 & \bar{\bar{A}}^T P-\bar{\bar{C}}^T U^T\\ * & \bar{\bar{D}}^T PP\bar{\bar{D}}-\mu I & \bar{\bar{D}}^T P\\ * & * & -P\end{bmatrix}<0, \tag{39}
$$

where

$$
\tilde{A}=\bar{\bar{A}}-\overline{\overline{KC}}, \tag{40}
$$

$$
\begin{aligned}
\tilde{A}^T P^T &= \left(\bar{\bar{A}}-\overline{\overline{KC}}\right)^T P \\
&=\bar{\bar{A}}^T P-\bar{\bar{C}}^T\bar{\bar{K}}^T P=\bar{\bar{A}}^T P-\bar{\bar{C}}^T U^T.
\end{aligned} \tag{41}
$$

The left-hand of (39) can be rewritten as

$$
\begin{aligned}
&\begin{bmatrix}\Omega & 0 & \bar{\bar{A}}^T P-\bar{\bar{C}}^T U^T\\ * & -\mu I & \bar{\bar{D}}^T P\\ * & * & -P\end{bmatrix} \\
&-\begin{bmatrix}\tilde{A}^T P & 0\\ 0 & \bar{\bar{D}}^T P\\ 0 & 0\end{bmatrix}\begin{bmatrix}-I & 0\\ 0 & -I\end{bmatrix}^{-1}\begin{bmatrix}P\tilde{A} & 0 & 0\\ 0 & P\bar{\bar{D}} & 0\end{bmatrix}<0.
\end{aligned} \tag{42a}
$$

Applying the Schur complement theorem to (42a), the inequality (39) becomes

$$
\begin{bmatrix}\Omega & 0 & \bar{\bar{A}}^T P-\bar{\bar{C}}^T U^T & \tilde{A}^T P & 0\\ * & -\mu I & \bar{\bar{D}}^T P & 0 & \bar{\bar{D}}^T P\\ * & * & -P & 0 & 0\\ * & * & * & -I & 0\\ * & * & * & * & -I\end{bmatrix}<0. \tag{42b}
$$

It is noticed that (42b) is the same as (30). Therefore, under the condition (30) or (42b), we have (38) holds. Therefore, in terms of (37) and (38), we can have

$$
\Delta V(k)\le-\frac{1}{\mu}\bar{e}^T(k)\bar{e}(k)+\mu\bar{\bar{d}}^T(k)\bar{\bar{d}}(k), \tag{43}
$$

$$
\begin{aligned}
\sum_{k=0}^{j}\Delta V(k)\le&-\frac{1}{\mu}\sum_{k=0}^{j}\bar{e}^T(k)\bar{e}(k) \\
&+\mu\sum_{k=0}^{j}\bar{\bar{d}}^T(k)\bar{\bar{d}}(k),\ \forall j>0.
\end{aligned} \tag{44}
$$

Under zero initial conditions, it is followed from (44)

$$
V(j+1)\le-\frac{1}{\mu}\sum_{k=0}^{j}\bar{e}^T(k)\bar{e}(k)+\mu\sum_{k=0}^{j}\bar{\bar{d}}^T(k)\bar{\bar{d}}(k). \tag{45}
$$

Therefore, we have

$$
\begin{aligned}
\frac{1}{\mu}\sum_{k=0}^{j}\bar{e}^T(k)\bar{e}(k)\le&\ \mu\sum_{k=0}^{j}\bar{\bar{d}}^T(k)\bar{\bar{d}}(k) \\
&-V(j+1)\le\mu\sum_{k=0}^{j}\bar{\bar{d}}^T(k)\bar{\bar{d}}(k),
\end{aligned} \tag{46}
$$

which means $\bar{e}(k)_2<\mu\bar{\bar{d}}(k)_2$ immediately. □

Remark 2: In the literature [28,32], augmented systems approach and unknow input observers were combined to achieve a robust fault estimation by decoupling unknown input uncertainties. Specifically, the paper [28] handled a dynamic system with partially decoupled unknown input uncertainties, which is technique for continuous dynamic system. The paper [32] was developed for discrete-time dynamic systems, which required the unknown input disturbance to meet decoupling condition. In the technique in Theorem 2 of this study, the unknow input disturbance does not need to meet the decoupling condition, where the disturbance is attenuated by using linear matrix inequality technique. More specifically, μ can be minimised by solving the matrix inequality (30) to reduce the effect of the external disturbance on the fault estimation and achieve a robust estimation of actuator faults and sensor faults.

4. SIMULATION STUDY

4.1. Simulation study on the drive train subsystem in a 4.8 MW wind turbine

In this section, the schematic figure of the 4.8 MW wind turbine system is shown by Fig. 1, from which one can see the wind turbine consists of four subsystems: blade and pitch system, drive train system, generator and converter, and controller. The parameter definition is as follows: v_w is the wind speed acting on the blade; τ_r is the rotor torque; τ_g is the generator torque; ω_r is the rotor speed; ω_g is the generator speed; β_r is the pitch position reference; β_m is the measured pitch position; $\omega_{r,m}$ is the measured rotational speed of the rotor; $\omega_{g,m}$ is the measured speed of the generator; $\tau_{g,m}$ is the measured generator torque; $\tau_{g,r}$ is the generator torque reference; P_r is the power reference; and P_g is the power generated by the generator. The wind turbine controller works in two modes [33,34]: (a) Control mode 1: set $\beta_r = 0$ so that the wind turbine works in power optimization region. (b) Control mode 2: set the controller as a PI controller so that the wind turbine works in power reference following region.

In this study, the drive train system of the 4.8 MW wind turbine is considered to demonstrate the effectiveness of the proposed method. The state space equation of the drive train system can be represented by [33]

$$J_r\dot{\omega}_r(t) = \tau_r(t) - K_{dt}\theta_\Delta(t) - (B_{dt}+B_r)\omega_r(t) + \frac{B_{dt}}{N_g}\omega_g(t), \tag{47}$$

$$J_g\dot{\omega}_g(t) = \frac{\eta_{dt}K_{dt}}{N_g}\theta_\Delta(t) + \frac{\eta_{dt}B_{dt}}{N_g}\omega_r(t) - \left(\frac{\eta_{dt}B_{dt}}{{N_g}^2} + B_g\right)\omega_g(t) - \tau_g(t), \tag{48}$$

$$\dot{\theta}_\Delta(t) = \omega_r(t) - \frac{1}{N_g}\omega_g(t), \tag{49}$$

where J_r is the moment of inertia of the low-speed shaft, J_g is the moment of inertia of the high-speed shaft, B_g and B_r are the friction coefficients of the high-speed and low-speed shafts, respectively, B_{dt} is the torsional damping coefficient, K_{dt} is the torsional stiffness, N_g is the gear ratio, η_{dt} is the efficiency of the drive train, $\theta_\Delta(t)$ is the torque angle of the drive train. The system parameter values of the drive train system used in this paper are taken from the paper [33], as shown in Table 1.

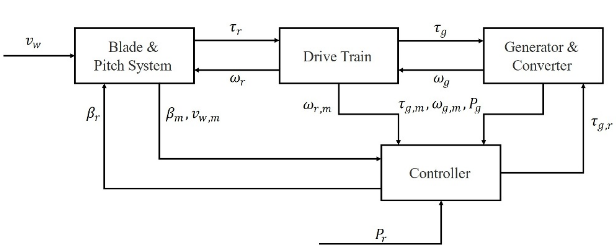

Fig. 1. Block-diagram of the wind turbine benchmark model from [34], redrawn by the authors.

Table 1. Values of the drive train system parameters.

Parameter	Value
J_r	55×10^6 kg·m^2
B_r	$7.11\ \frac{\text{Nms}}{\text{rad}}$
B_{dt}	$775.49\ \frac{\text{Nms}}{\text{rad}}$
N_g	95
J_g	390 kg·m^2
B_g	$45.6\ \frac{\text{Nms}}{\text{rad}}$
K_{dt}	$2.7\times10^9\ \frac{\text{Nms}}{\text{rad}}$
η_{dt}	0.97

Substituting the parameters in Table 1 into the wind turbine drive train system (47)-(49) and discretizing them, the parameter matrix of the linear discrete system in the form of (1) can be obtained as follows:

$$A = \begin{bmatrix} 0.9976 & 0.0000 & -0.4844 \\ 3.5099 & 0.9619 & 697.1662 \\ 0.0099 & -0.0001 & 0.9606 \end{bmatrix},$$

$$B = 10^{-4}\times\begin{bmatrix} 0.0000 & -0.0000 \\ 0.0000 & -0.2531 \\ 0.0000 & 0.0000 \end{bmatrix},\ C = \begin{bmatrix} 1 & 0 & 0 \\ 0 & 1 & 0 \end{bmatrix},$$

$$E_a = 10^{-4}\times\begin{bmatrix} -0.0000 \\ -0.2531 \\ 0.0000 \end{bmatrix},\ E_s = \begin{bmatrix} 1 \\ 0 \end{bmatrix},$$

and the state vector is $x = \begin{bmatrix} \omega_g & \omega_r & \theta_\Delta \end{bmatrix}^T$.

The second actuator has 1% effectiveness loss from 2500 seconds to 3500 seconds. The first sensor has sinusoidal disruption after 1000 seconds, that is,

$$f_s(t) = \begin{cases} 0.1\sin(0.008t), & t \ge 1000, \\ 0, & \text{else}. \end{cases} \tag{50}$$

We use the proposed discrete-time observer in the form of (8)-(10) with the sample time 0.01 seconds. The observer gain below is chosen so that the estimation error dynamics is stable

$$L = \begin{bmatrix} -0.0000 & -0.0001 \\ -0.0003 & 1.9861 \\ -0.0000 & 0.0014 \\ 0.0082 & -43.5509 \end{bmatrix},\ K = \begin{bmatrix} 1.0000 & -0.0006 \end{bmatrix}. \tag{51}$$

The simulation is run for 4900 seconds. Figs. 2 and 3 show the states ω_g and ω_r (blue solid lines) of the wind turbine drive train system and their estimates (red dotted lines) under faulty conditions. The results reveal that the estimates obtained by this algorithm can accurately track

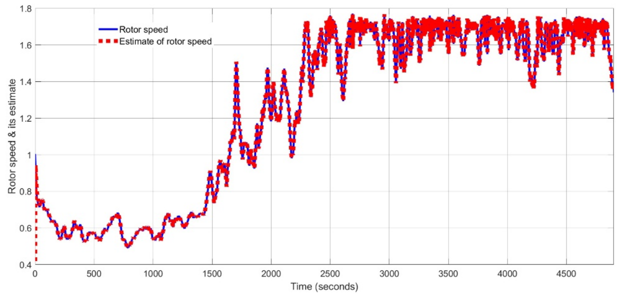

Fig. 2. Rotor speed and its estimate.

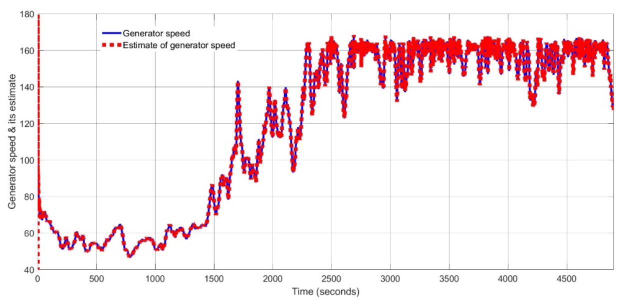

Fig. 3. Generator speed and its estimate.

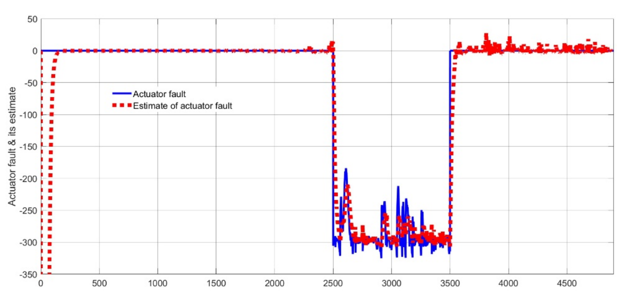

Fig. 4. Second actuator fault and its estimation.

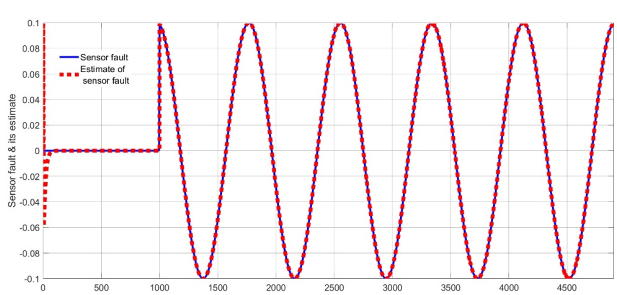

Fig. 5. First sensor fault and its estimation.

the actual states. The actuator and sensor fault and their estimates are depicted by Figs. 4 and 5, from which one can see the fault signals are successfully reconstructed. By observing the estimated fault signals, we can clearly identify the time when the faults occur and determine the size and shape of the faults. Although the occurring time-interval of the two faults have overlapped, and the types of the two faults are different, the tracking performance of the proposed estimator is excellent.

4.2. Simulation study on an electromechanical servo system

In this section, an electromechanical servo system is considered to demonstrate the effectiveness of the proposed algorithm. The model can be described by the Lipschitz nonlinear system [35]

$$x(k+1) = \underbrace{\begin{bmatrix} 0.0468 & 0.1564 \\ 0.2083 & 0.8154 \end{bmatrix}}_{A} \begin{bmatrix} x_1(k) \\ x_2(k) \end{bmatrix} + \underbrace{\begin{bmatrix} 39.2076 \\ 11.5299 \end{bmatrix}}_{B} u(k) + \psi(x(k), u(k)) + E_a f_a(k) + Dd(k), \tag{52}$$

$$y(k) = \underbrace{\begin{bmatrix} 1 & 0 \\ 0 & 1 \end{bmatrix}}_{C} \begin{bmatrix} x_1(k) \\ x_2(k) \end{bmatrix} + E_s f_s(k). \tag{53}$$

$x_1(k)$ and $x_2(k)$ are the load angular position and the shaft speed, respectively. The input voltage $u(k) = 2.5$, $\psi(x(k), u(k)) = [0, -0.005\sin(x_1(k))]^T$, and the sampling time is 0.1 seconds.

The distribution matrices are considered as follows:

$$D = \begin{bmatrix} 0.1 \\ 0 \end{bmatrix},\ E_a = B, E_s = \begin{bmatrix} 1 \\ 0 \end{bmatrix}. \tag{54}$$

Choosing $\gamma = 0.005$, and $\mu = 180$, one can solve (30) in Theorem 2 to yield

$$L = \begin{bmatrix} 1.0637 & 0.2894 \\ 0.4916 & 0.9194 \\ 0.0260 & 0.0030 \end{bmatrix},\ K = \begin{bmatrix} 0.0739 & -0.3372 \end{bmatrix}. \tag{55}$$

The actuator fault is the discrete-time signal given as follows:

$$f_a(k) = \begin{cases} 0.5\sin(0.2\pi k), & 5 \le k < 10, \\ -0.125k + 0.5\sin(0.2\pi k), & 10 \le k < 12, \\ -0.1(k-12)^2 + 0.5\sin(0.2\pi k), & 12 \le k < 15, \\ 0, & \text{else.} \end{cases} \tag{56}$$

The input disturbance signal is assumed to be

$$d(k) = 0.1\sin(50\pi k). \tag{57}$$

In the discrete-time signals above, k means kT actually where T is the sampling time and k is an integer.

The first sensor is assumed to have 25% effectiveness loss in the measurement after 25 seconds.

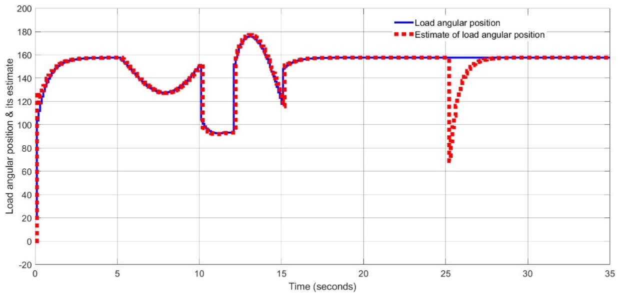

Fig. 6. The load angular position and its estimate.

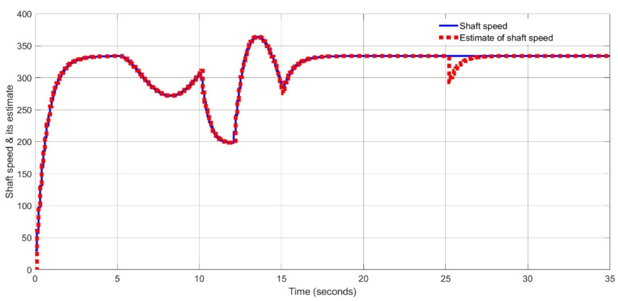

Fig. 7. The shaft speed and its estimate.

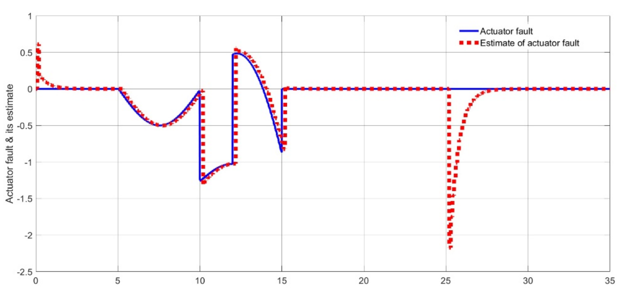

Fig. 8. Actuator fault and its estimate.

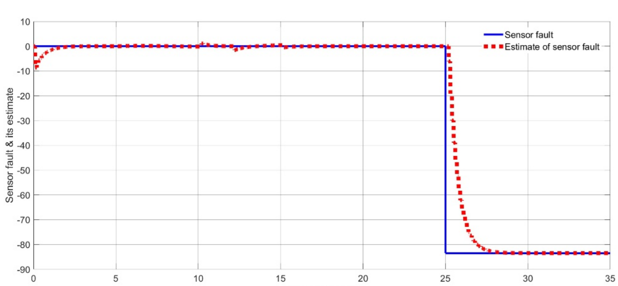

Fig. 9. Sensor fault and its estimation.

Figs. 6 and 7 show the system states and their estimates, from which one can see the tracking performance is satisfactory. The effects from the actuator fault on the system states are significant which are clearly visible. The sensor faults occurring at 25 seconds make the estimated curves have dips, but the estimated curves recover shortly, achieving a robust state estimate. The actuator and sensor faults and their estimates are shown in Figs. 8 and 9. It is noted that the sensor faults occurring at 25 seconds make the estimated curve of the actuator fault has an instant drop but the estimated curve recovers tracking within 2.5 seconds, which is excellent. The effect of the actuator fault on the estimate of sensor fault is negligible, therefore, the estimation performance of the sensor fault is satisfactory.

5. CONCLUSION

A technique for simultaneous estimation of state and multiple faults has been addressed which can be used for both linear and Lipschitz nonlinear discrete systems corrupted by unknown input disturbances. Based on Lyapunov stability theorem, the condition of estimation error stability has been analyzed, the unknown input disturbance can be attenuated by using LMI technology to seek an optimal observer gain to ensure the estimation robustness. Simultaneous state and fault estimation can be realized by combining augmented system approach and proportional integral observer technique. Two engineering-oriented systems (wind turbine drive system and electromechanical servo system) have been used to verify the feasibility of the proposed design. The techniques of this study are developed for discrete-time systems, which more suit real-time applications of various engineering systems including wind turbine systems and electromechanical servo systems.

The proposed simultaneous state and fault estimation technique would be applied to the fault diagnosis for electric vehicles [36] and extended to engineering systems with high nonlinearities such as complex robotic systems [37] and offshore energy systems [38], which could be potential topics for further research.

CONFLICT OF INTEREST

The authors declare that there is no competing financial interest or personal relationship that could have appeared to influence the work reported in this paper.

REFERENCES

[1] Z. Gao, C. Cecati, and S. X. Ding, "A survey of fault diagnosis and fault-tolerant techniques—part I: Fault diagnosis with model-based and signal-based approaches," *IEEE Transactions on Industrial Electronics*, vol. 62, no. 6, pp. 3757-3767, 2015.

[2] S. Lu, Z. Gao, P. Zhang, Q. Xu, T. Xie, and A. Zhang, "Event-triggered federated learning for fault diagnosis of offshore wind turbines with decentralized data," *IEEE Transactions on Automation Science and Engineering*, vol. 21, no. 2, pp. 1271-1283, 2024.

[3] P. Frank, "Fault diagnosis in dynamic systems using analytical and knowledge-based redundancy - A survey and some new results," *Automatica*, vol. 26, no. 3, pp. 459-474, 1990.

[4] J. Chen and R. Patton, *Robust Model-based Fault Diagnosis for Dynamic Systems*, Kluwer, Boston, MA, USA, 1999.

[5] Z. Gao and D. Ho, "Proportional multiple-integral observer design for descriptor systems with measurement output disturbances," *Proceedings of IEE Control Theory and Applications*, vol. 151, no. 3, pp. 279-288, 2004.

[6] Z. Gao and H. Wang, "Descriptor observer approaches for multivariable systems with measurement noises and application in fault detection and diagnosis," *Systems and Control Letters*, vol. 55, no. 4, pp. 304-313, 2006.

[7] C. Huang, F. Naghdy, and H. Du, "Delta operator-based fault estimation and fault-tolerant model predictive control for steer-by-wire systems," *IEEE Transactions on Control Systems Technology*, vol. 26, no. 5, pp. 1810-1817, 2018.

[8] M. Liu and P. Shi, "Sensor fault estimation and tolerant control for Itô stochastic systems with a descriptor sliding mode approach," *Automatica*, vol. 49, no. 5, pp. 1242-1250, 2013.

[9] X. Chu and M. Li, "Event-triggered fault estimation and sliding mode fault-tolerant control for a class of nonlinear networked control systems," *Journal of the Franklin Institute*, vol. 355, no. 13, pp. 5475-5502, 2018.

[10] H. Alwi and C. Edwards, "Robust fault reconstruction for linear parameter varying systems using sliding mode observers," *International Journal of Robust and Nonlinear Control*, vol. 24, no. 14, pp. 1947-1968, 2014.

[11] M. Rodrigues, H. Hamdi, D. Theilliol, C. Mechmeche, and N. B. Braiek, "Actuator fault estimation based adaptive polytopic observer for a class of LPV descriptor systems," *International Journal of Robust and Nonlinear Control*, vol. 25, no. 5, pp. 673-688, 2015.

[12] J. Han, H. Zhang, Y. Wang, and K. Zhang, "Fault estimation and fault-tolerant control for switched fuzzy stochastic systems," *IEEE Transactions on Fuzzy Systems*, vol. 26, no. 5, pp. 2993-3003, 2018.

[13] B. Li, W. Dong, W. Xie, and J. Chang, "Robust control for super-maneuver flight based on adaptive observer," *Proc. of Chinese Control & Decision Conference (CCDC)*, IEEE, pp. 22-27, 2018.

[14] M. Witczak, D. Rotondo, V. Puig, F. Nejjari, and M. Pazera, "Fault estimation of wind turbines using combined adaptive and parameter estimation schemes," *International Journal of Adaptive Control and Signal Processing*, vol. 32, no. 4, pp. 549-567, 2018.

[15] A. Abbaspour, P. Aboutalebi, K. K. Yen, and A. Sargolzaei, "Neural adaptive observer-based sensor and actuator fault detection in nonlinear systems: Application in UAV," *ISA Transactions*, vol. 67, pp. 317-329, 2017.

[16] L. Chen, C. Edwards, and H. Alwi, "Sensor fault estimation using LPV sliding mode observers with erroneous scheduling parameters," *Automatica*, vol. 101, pp. 66-77, 2019.

[17] K. Veluvolu, M. Defoort, and Y. Soh, "High-gain observer with sliding mode for nonlinear state estimation and fault reconstruction," *Journal of the Franklin Institute*, vol. 351, no. 4, pp. 1995-2014, 2014.

[18] Z. Gao, T. Breikin, and H. Wang, "Discrete-time proportional and integral observer and observer-based controller for systems with both unknown input and output disturbances," *Optimal Control Applications and Methods*, vol. 29, no. 3, pp. 171-189, 2008.

[19] M. Do, D. Koenig, and D. Theilliol, "Robust H_∞ proportional-integral observer for fault diagnosis: Application to vehicle suspension," *IFAC-PapersOnLine*, vol. 51, no. 24, pp. 536-543, 2018.

[20] Z. Gao, S. Ding, and Y. Ma, "Robust fault estimation approach and its application in vehicle lateral dynamic systems," *Optimal Control Applications and Methods*, vol. 28, no. 3, pp. 143-156, 2007.

[21] X. Liu and Z. Gao, "Robust finite-time fault estimation for stochastic nonlinear systems with Brownian motions," *Journal of The Franklin Institute*, vol. 354, no. 6, pp. 2500-2523, 2017.

[22] Z. Gao, T. Breikin, and H. Wang, "High-gain estimator and fault-tolerant design with application to a gas turbine dynamic system," *IEEE Transactions on Control Systems Technology*, vol. 15, no. 4, pp. 740-753, 2007.

[23] Z. Gao, "Estimation and compensation for Lipschitz nonlinear discrete-time systems subjected to unknown measurement delays," *IEEE Transactions on Industrial Electronics*, vol. 62, no. 9, pp. 5950-5961, 2015.

[24] A. Jmal, O. Naifar, A. Makhlouf, N. Derbel, and M. Hammami, "Sensor fault estimation for fractional-order descriptor one-sided Lipschitz systems," *Nonlinear Dynamics*, vol. 91, no. 3, pp. 1713-1722, 2017.

[25] M. Kazemi and M. Montazeri, "A new fault detection approach for nonlinear Lipschitz systems with optimal disturbance attenuation level and Lipschitz constant," *Electrical Engineering*, vol. 100, no. 3, pp. 1997-2009, 2018.

[26] J. Zhang, A. Swain, and S. Nguang, "Simultaneous robust actuator and sensor fault estimation for uncertain nonlinear Lipschitz systems," *IET Control Theory & Applications*, vol. 8, no. 14, pp. 1364-1374, 2014.

[27] M. Defoort, K. Veluvolu, J. Rath, and M. Djemai, "Adaptive sensor and actuator fault estimation for a class of uncertain Lipschitz nonlinear systems," *International Journal of Adaptive Control and Signal Processing*, vol. 30, no. 2, pp. 271-283, 2016.

[28] Z. Gao, X. Liu, and M. Chen, "Unknown input observer-based robust fault estimation for systems corrupted by partially decoupled disturbances," *IEEE Transactions on Industrial Electronics*, vol. 63, no. 4, pp. 2537-2547, 2015.

[29] J. Chang, "Applying discrete-time proportional integral observers for state and disturbance estimations," *IEEE Transactions on Automatic Control*, vol. 51, no. 5, pp. 814-818, 2006.

[30] Z. Gao, "Fault estimation and fault tolerant control for discrete-time dynamic systems," *IEEE Transactions on Industrial Electronics*, vol. 62, no. 6, pp. 3874-3884, 2015.

[31] Y. Gu and G. Yang, "Simultaneous actuator and sensor fault estimation for discrete-time Lipschitz nonlinear systems in finite-frequency domain," *Optimal Control Applications and Methods*, vol. 39, no. 1, pp. 410-423, 2018.

[32] E. Chaves Jr., A. de A. Dantas, and A. Maitelli, "Robust observer-based actuator and sensor fault estimation for discrete-time systems," *Journal of Control, Automation and Electrical Systems*, vol. 30, no. 2, pp. 160-169, 2019.

[33] R. Gao and Z. Gao, "Pitch control for wind turbine systems using optimization, estimation and compensation," *Renewable Energy*, vol. 91, pp. 505-515, 2016.

[34] P. Odgaard, J. Stoustrup, and M. Kinnaert, "Fault-tolerant control of wind turbines: A benchmark model," *IEEE Transactions on control systems Technology*, vol. 21, no. 4, pp. 1168-1182, 2013.

[35] Z. Gao, "Estimation and compensation for Lipschitz nonlinear discrete-time systems subjected to unknown measurement delays," *IEEE Transactions on Industrial Electronics*, vol. 62, no. 9, pp. 5950–5961, 2015.

[36] T. Lan, Z.-W. Gao, H. Yin, and Y. Liu, "A sensor-fault-estimation method for lithium-ion batteries in electric vehicles," *Sensors*, vol. 23, no. 18, 7737, 2023.

[37] O. Elhaki, K. Shojaei, A. Mohammadzadeh, and S. Rathinasamy, "Robust amplitude-limited interval type-3 neuro-fuzzy controller for robot manipulators with prescribed performance by output feedback," *Neural Computing and Applications*, vol. 35, no. 12, pp. 9115-9130, 2023.

[38] R. Manikandan, R. Sakthivel, and M. Chadli, "Non-linear control design for optimized power regulations in spar wind turbines under wind and wave loads," *Ocean Engineering*, vol. 266, no. 4, 112916, 2022.

Zikang Li received his B.S. degree in robotics engineering from Wuhan Business University in 2021. He is now a postgraduate student in Northeast Petroleum University. His research interest is model-based fault estimation for discrete-time systems.

Zhi-Wei Gao is the Distinguished Professor, founder and director of Research Centre for Digitalization and Intelligent Diagnosis to New Energies at Northeast Petroleum University. His research interests include digital twins, industrial informatics security, and clean energy.

Yuanhong Liu received his B.S. and M.S. degrees from the School of Information and Electrical Engineering, Northeast Petroleum University, in 2003 and 2008, respectively. He received a Ph.D. degree from the Department of Control Science and Engineering, Harbin Institute of Technology, in 2016. His research interests include nonlinear dimension reduction, machine learning and pattern recognition, signal processing. Dr. Liu is the Associate Editor of IEEE Transactions on Industrial Informatics.